



Local Symmetry and Global Structure of Coronary Arterial Tree Models generated by Constrained Constructive Optimization

W. Schreiner, F. Neumann, M. Neumann, R. Karch

*Department of Medical Computer Sciences, Department of Cardiothoracic Surgery, Institute of Experimental Physics, University of Vienna, Spitalgasse 23, A-1090 Vienna, Austria
E-Mail: wolfgang.schreiner@akh-wien.ac.at*

Abstract

The procedure of Constrained Constructive Optimization (CCO) generates a binary branching model of vascular segments, represented as straight cylindrical tubes through which resistance to blood flow follows Poiseuille's Law. While several constraints regarding pressures, flows and branching radii are fulfilled throughout the optimization process, the branching structure is generated so as to convey blood to each site of a perfusion area, where it is delivered into the microcirculation. As every real arterial tree CCO-models also comprise a mixture of "conveying" and "delivering" elements of function. Since no anatomical information is plugged into CCO-models, the local and global structure solely results from the numerical optimization process. Different target functions as well as additional constraints can be examined regarding their impact on structural features. Likewise changes in constraints induce different structures of the model trees. In the present work we illustrate the impact of an additional local criterion applied to each new bifurcation generated, namely setting a lower limit to the ratio between the radii of smaller and larger daughter. Thus, precluding very asymmetric bifurcations was found to convert a CCO-model from a "conveying" to a "delivering" type of function, as reflected in the respective numerical indices.

Introduction

Vascular trees fulfill the crucial task of carrying blood to the tissue and removing metabolic endproducts therefrom. Many efforts have been made to gain a thorough understanding of the hemodynamic details of blood transport for both improved diagnosis and therapy. Over the last decade computer simulation has emerged as a potent tool to model blood flow, based on mechanical models of the respective arterial trees.

The first and most simple approach was a compartmental representation, where properties (resistances, compliances) of whole classes of vessel segments are lumped into several compartments (Bruinsma [1]). Evidently such models cannot represent details in structure and lend themselves only for obtaining global results. A second approach is the “anatomical” modeling (Rooz [2]) of small portions of arterial trees, where topographic information is directly represented by corresponding models of arterial segments. These models are “accurate” in detail, they cannot represent the complete vascular system of an organ, however. A third approach, namely self similar arterial tree models offer detailed structures which also reproduce the features of real arterial trees in a statistical sense (West [3], Pelosi [4], Dawant [5], Levin [6]). However, the geometrical arrangement of vessel segments in these “fractal” models follows *ab initio* rules rather than being adapted to the physiological needs of blood supply.

We therefore established a new method of generating dichotomously branching models for arterial trees combining the benefits of the approaches discussed above. This method, called **Constrained Constructive Optimization (CCO)**, starts from first principles:

- Blood should be distributed as evenly as possible over the whole part of tissue to be perfused.
- A given pressure (p_{term}) should be available to perfuse the microcirculation distal to the CCO-model.
- At each bifurcation the radii of vessel segments should fulfill a “bifurcation law” adapted to results found in real arterial trees (Arts [7], Zamir [8], Sherman [9], Zamir [10]). We choose $\gamma = 2.55$ for the so called “bifurcation exponent” (Zamir [11], Zamir [12]).
- Structure and geometry of the CCO-model tree should be designed such that a given optimization target function, being calculated from the model tree as a whole, is minimized (Thompson [13], Cohn [14], Cohn [15], Zamir [16], Lefevre [17], In the present work we select total intravascular volume as optimization target (Sherman [9], Kamiya [18]).

In principle, CCO generates the model tree by successively adding new terminal segments while preserving all constraints throughout the process of model growth. Each step of growth is governed by geometrical optimization nested within structural optimization, both types of optimization being performed according to the same target function. Details of the method and the algorithm have been reported in previous papers (Schreiner [19], Schreiner [20]) and are also given in another article within the current volume (Neumann [21]).

Imposing an additional constraint to CCO

In “pure CCO” only the relation between radii is governed by a bifurcation law which each bifurcation is required to fulfill identically. In nature, however, there is also an absolute lower limit for segment radii (capillary radius). Given the maximum segment radius occurring in the tree, this implies an absolute lower bound for the symmetry index

$$\xi_{\text{rad}} = r_2/r_1 \quad (1)$$

where r_2 and r_1 represent the radii of the small and large daughter segments ($r_2 \leq r_1$). Very asymmetric bifurcations have symmetry indices closed to 0, whereas a perfectly symmetric bifurcation is characterized by $\xi_{\text{rad}} = 1$. Moreover, measurements of corrosion casts (van Bavel [22], Aharinejad [23]), indicate that the maximum possible asymmetry namely

$$\xi_{\text{rad}} = r_{\text{min}}/r_{\text{max}} \quad (2)$$

usually does not occur in reality since the root segment of a tree (r_{max}) very unlikely gives rise to the smallest daughter segment (r_{min}) (this could only happen by coincidence). In reality bifurcations are rather much more symmetric, and symmetry indices smaller than $\xi_{\text{rad}} = 0.05$ are practically never encountered.

Every model of arterial trees has to reduce complexity by limiting the total number of segments in the model. This can be achieved either by truncating at a certain bifurcation order or by limiting the number of terminal segments considered (N_{term}); in a binary branching tree the total number of segments N_{tot} is always given by

$$N_{\text{tot}} = 2 \cdot N_{\text{term}} - 1 \quad (3)$$

In the present work we generated trees for given $N_{\text{term}} = 4000$. Since the models represent only a portion of the real arterial tree, the maximum bifurcation-asymmetry occurring in the model should match that of the corresponding portion of the real tree.

128 Simulations in Biomedicine IV

As a consequence, in the present work CCO will be performed with an additional limit ξ^{low} imposed on new bifurcations generated. Each new bifurcation tentatively generated is accepted only on the condition that

$$\xi_{\text{rad}} > \xi^{\text{low}}, \quad (4)$$

otherwise the connection is precluded from becoming permanent.

Apart from the additional limit on asymmetry the algorithm of CCO is performed as usual, creating an optimized model of the arterial tree which simultaneously conforms to all constraints.

Results

Visual appearance

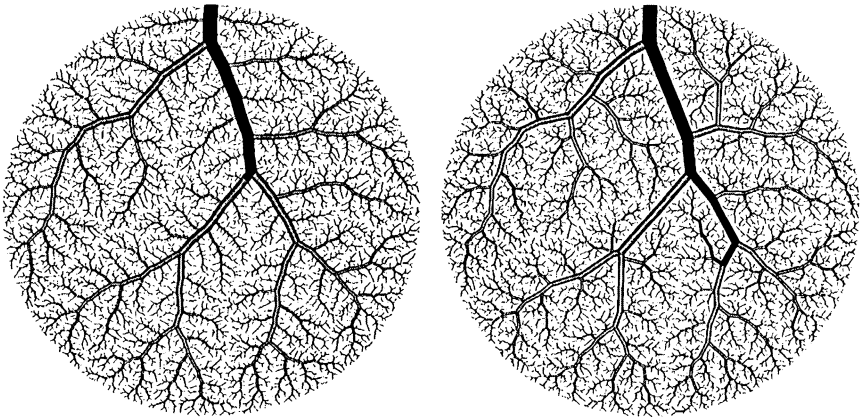


Figure 1: Structural changes of CCO-generated arterial tree models due to a limit to asymmetry

Both trees were generated with identical constraints and the optimization target was minimum intravasal volume. Compared to the unrestricted tree in the left panel it is evident from the right panel how the restriction on local bifurcation asymmetry changes the global topological and geometrical structure. Note the full circular marker at the site of perfusion to which we refer in the text.

Left Panel: $\xi^{\text{low}} = 0$ (unlimited asymmetry)

Right Panel: $\xi^{\text{low}} = 0.4$

First we illustrate the effect of limiting local bifurcation asymmetry on the visual appearance of the model trees. Since the most asymmetric bifurcations

occur when a mainstream segment gives off a small branch, we pick such a bifurcation from a CCO tree generated without a limit on asymmetry and focus on the terminal site supplied by the small branch, see Figure 1 left panel for

$\xi^{\text{low}} = 0$: Without restriction of asymmetry the microcirculatorial area is supplied via a tiny side branch emerging directly from the right major branch (note that the bifurcation from the major branch into this side branch has a very low value of ξ_{rad}), resulting in a very direct access to the site of supply.

As opposed to that not only the global structure but also the path of access changes drastically when imposing

$\xi^{\text{low}} = 0.4$: With this very severe restriction, a large portion of bifurcations of the tree are forced to be “more symmetric”. The very basic and dramatic changes induced in global structure may in fact be seen as a “switch in topology”. In particular, the terminal site on which we have focused above, is now supplied via a totally different subtree emerging from the left (instead of the right) major branch. (Please note that “right” and “left” refers to the direction of blood flow.) The former route of supply is no longer feasible, since the small segment cannot branch off directly from a major segment any longer. Instead, a new subtree has emerged far more distally.

The specific example clearly illustrates how **local restrictions** on asymmetry can entail **global changes in structure**. In the following we shall provide quantitative estimators for the effects intuitively characterized above.

Changes in global quantities due to limited bifurcation asymmetry

For any optimization process, imposing an additional limit means to worsen the optimum value of the target function achieved. Specifically, optimizing for total intravasal volume will result in a larger intravasal volume with the constraint (limited bifurcation asymmetry) being added. The more the constraint is tightened (i.e. for increasing ξ^{low}) the more increases the “minimum” volume. Nine trees have been generated using identical constraints and target functions but increasing values of ξ^{low} , the concomitant increase in volume being displayed in Figure 2. The severe limit on asymmetry makes the volume increase by approximately 10 %.

While the increase in volume (which is also the optimization target) is a necessary consequence of **any** additional restriction to optimization, the increases observed for total vascular surface and the radius of the root segment are findings of the present work. They are not unexpected, however, since the formulae for volume and surface differ only by a factor $2 \cdot r$.

130 Simulations in Biomedicine IV

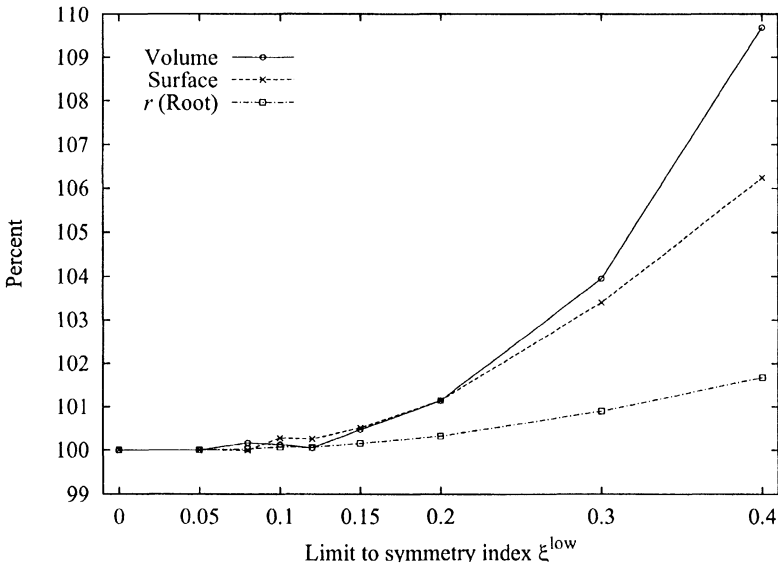


Figure 2: Dependence of global quantities on the limit to asymmetry

x-axis: limit to asymmetry (ξ^{low} , [dimensionless]).

y-axis: percentage relative to reference tree ($\xi^{\text{low}} = 0$). Total intravascular volume of tree, shown as circles, total surface of vessels in the model tree, shown as crosses and radius of root segment shown as squares.

Note that this figure also displays the results for additional CCO-trees with $\xi^{\text{low}} = 0.05, 0.08, 0.1, 0.12, 0.14, 0.2$, and 0.3 , besides the two trees shown in Figure 1 ($\xi^{\text{low}} = 0$ and 0.4).

The increase in the root radius is plausible when considering the fact that massive detours induced by the limit to asymmetry increase the total lengths of segments; since overall resistance must remain constant, radii have to increase. In fact the joint effect of the increase in surface and radii accounts for the increase in total volume.

Changes in the frequency distribution of symmetry indices

As second approach to quantify the structural changes due to the additional constraint on local asymmetry is based on the frequency distribution of ξ_{rad} , obtained for the whole tree (cf. Figure 3). First of all we notice that almost symmetric bifurcations (ξ_{rad} close to 1) occur in all trees with similar probability densities, they do not contribute the majority of segments, however. Slightly asymmetric bifurcations are more frequent, with the modal value (i.e. the value with maximum probability) occurring between $0.4 \leq \xi_{\text{rad}} \leq 0.5$. Bifurcations

even more asymmetric become less frequent and each distribution approaches zero somewhere between $0.05 \leq \xi_{\text{rad}} \leq 0.2$. Evidently the minimum value of ξ_{rad} found in a tree is determined by the constraint ξ^{low} : as ξ^{low} increases, the minimum ξ_{rad} and bifurcations with low ξ_{rad} are shifted towards the right, and the corresponding trees show higher values for the probability density in the region $\xi_{\text{rad}} \geq 0.5$.

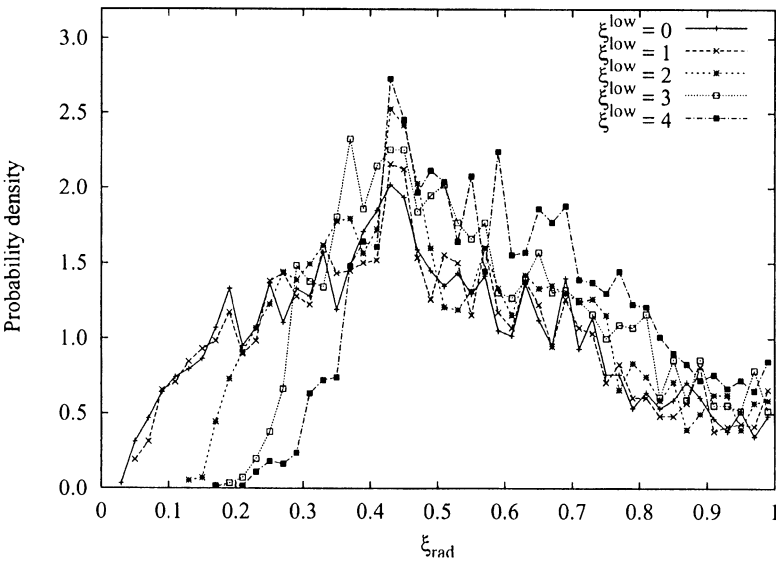


Figure 3: Probability density of symmetry index

x-axis: symmetry index (ξ_{rad} , [dimensionless]) according to Eq. 1.

y-axis: estimated probability density. All trees have 4000 terminal segments and are optimized for minimum intravasal volume. Note that each (of the 3999) bifurcating segment(s) has a symmetry index, whereas terminal segments have none. Solid line: $\xi^{\text{low}} = 0$, i.e. a tree without restriction. See the legend for the other values of $\xi^{\text{low}} = 0.1, 0.3, 0.4$, two of them corresponding to the trees shown in Figure 1.

There is an interesting detail noticeable namely that minimum values of ξ_{rad} turn out to be smaller than the corresponding limit ξ^{low} . This apparent contradiction has a natural explanation: When adding a new bifurcation the limit cannot be violated by definition. However, the tree proximal to any new segment is rescaled so as to reestablish boundary conditions and constraints after including the new segment. Thereby segment radii (and also their ratios) may change at bifurcations due to their location. This may well lead to a “post hoc” violation of the ξ^{low} -constraint which, by definition, is not applied to “existing” bifurcations.



Summary

CCO generates the structure and geometry of arterial tree models without drawing on any information from topographic anatomy. Yet the models resemble real coronary arterial trees in many features, as discussed and evaluated in previous reports (Schreiner [19], Schreiner [24], Schreiner [25]). However, the existence of very small side branches emerging from big vessels is conspicuous (Figure 1, left panel) when compared with real coronary trees, where these structures are rarely found. Therefore we added an additional constraint to CCO by limiting the asymmetry of any new bifurcation when the tree is generated. The resulting changes in structure are not only obvious to visual inspection (detours emerge as a consequence of avoiding highly asymmetric bifurcations, see Figure 1, right panel) but can also be quantified by a set of statistical descriptors. We examined three global quantities, namely the total volume, the total surface, and the radius of the root segment of the tree. All of them increase when tightening the limit to asymmetry. We also showed the impact on the frequency distribution of the symmetry indices found throughout the tree.

The main goal of the present work was to demonstrate how **a locally applied constraint is able to induce global structural changes** in an optimized arterial tree model.

Acknowledgments

This work was supported by the Bundesministerium für Wissenschaft und Forschung, grant 49.820/4-24/92. The authors wish to thank Mrs. E. Sumetzberger for preparing the manuscript.

References

Bruinsma, P., Arts, T., Spaan, J.A.E. Coronary pressure flow characteristics in relation to the distensibility of microvessels, *Med. Biol. Eng. and Comp.*, 1985, **23** suppl II, 1325-1326.



Roos, E., Wiesner, T.F., Nerem, R.M. Epicardial coronary blood flow including the presence of stenosis and aorto-coronary bypasses - I: Model and numerical method, *ASME J. Biomech. Eng.*, 1985, **107**, 361-367.

West, B.J. & Goldberger, A.L. Physiology in fractal dimensions, *Am. Sci.*, 1987, **75**, 354-364.

Pelosi, G., Saviozzi, G., Trivella, M.G., L'Abbate, A. Small artery occlusion: A theoretical approach to the definition of coronary architecture and resistance by a branching tree model, *Microvasc. Res.*, 1987, **34**, 318-335.

Dawant, B., Levin, M., Popel, A.S. Effect of dispersion of vessel diameters and lengths in stochastic networks I. Modeling of microcirculatory flow, *Microvasc. Res.*, 1985, **31**, 203-222.

Levin, M., Dawant, B., Popel, A.S. Effect of dispersion of vessel diameters and lengths in stochastic networks II. Modeling of microvascular hematocrit distribution, *Microvasc. Res.*, 1986, **31**, 223-234.

Arts, T., Kruger, R.T.I., van Gerven, W., Lambregts, J.A.C., Reneman, R.S. Propagation velocity and reflection of pressure waves in the canine coronary artery, *Am. J. Physiol.*, 1979, **237**, H469-H474.

Zamir, M. Distributing and delivering vessels of the human heart, *J. Gen. Physiol.*, 1988, **91**, 725-735.

Sherman, T.F. On connecting large vessels to small: The meaning of MURRAY's law, *J. Gen. Physiol.*, 1981, **78**, 431-453.

Zamir, M. Shear forces and blood vessel radii in the cardiovascular system, *J. Gen. Physiol.*, 1977, **69**, 449-461.

Zamir, M. & Chee, H. Segment analysis of human coronary arteries, *Blood Vessels*, 1987, **24**, 76-84.

Zamir, M. & Chee, H. Branching characteristics of human coronary arteries, *Can. J. Physiol. Pharmacol.*, 1986, **64**, 661-668.

Thompson, D.W. *On growth and form. Volume II.*, University Press, Cambridge, 1952.

Cohn, D.L. Optimal systems: I. The vascular system, *Bull. Math. Biophys.*, 1954, **16**, 59-74.



134 Simulations in Biomedicine IV

Cohn, D.L. Optimal systems: II. The cardiovascular system, *Bull. Math. Biophys.*, 1955, **17**, 219-227.

Zamir, M. & Bigelow, D.C. Cost of departure from optimality in arterial branching, *J. theor. Biol.*, 1984, **109**, 401-409.

Lefevre, J. Teleonomical representation of the pulmonary arterial bed of the dog by a fractal tree, *Cardiovascular system dynamics: Models and measurements*, eds. T. Kenner, R. Busse, H. Hinghofer-Szalkay pp 137-146, Plenum Press, New York, London, 1982.

Kamiya, A. & Togawa, T. Optimal branching structure of the vascular tree, *Bull. Math. Biophys.*, 1972, **34**, 431-438.

Schreiner, W. & Buxbaum, P.F. Computer-optimization of vascular trees, *IEEE Trans. Biomed. Eng.*, 1993, **40**, 482-491.

Schreiner, W. Computer generation of complex arterial tree models, *J. Biomed. Eng.*, 1993, **15**, 148-150.

Neumann, F., Schreiner, W., Karch, R., Neumann, M. Structure of computer-generated arterial trees with different optimization target functions, *BIOMED 97*, 1997.

van Bavel, E. & Spaan, J.A.E. Branching patterns in the porcine coronary arterial tree Estimation of flow heterogeneity, *Circ. Res.*, 1992, **71**, 1200-1212.

Aharinejad, S.H., Schreiner, W., Neumann, F. Morphometry of human coronary arterial trees, *Microvasc. Res.*, 1996. In press.

Schreiner, W., Neumann, M., Neumann, F., Roedler, S.M., End, A., Buxbaum, P.F., Müller, M.R., Spieckermann, P. The branching angles in computer-generated optimized models of arterial trees, *J. Gen. Physiol.*, 1994, **103**, 975-989.

Schreiner, W., Neumann, F., Neumann, M., End, A., Roedler, S.M., Aharinejad, S.H. The influence of optimization target selection on the structure of arterial tree models generated by constrained constructive optimization, *J. Gen. Physiol.*, 1995, **106**, 583-599.